Chapter 1

Introduction

1.1 Introduction

Einsteins theory of general relativity (GR) [Einstein, 1915b,a, de Sitter, 1917, Silberstein, 1917] together with quantum field theory are considered to be the pillars of modern physics. GR deals with gravitational phenomena treating space-time as a four-dimensional manifold. The theory has a well understood and mathematically very elegant structure and is internally consistent. GR describes gracefully all the experimental tests of gravity [Weinberg, 1972, Berti et al., 2015] conducted till now without a single adjustable parameter.

1.2 General Relativity

The inverse-square gravitational force law introduced by Newton predicted correctly a variety of gravitational phenomena including planetary motion. In fact the

Newtons theory was very successful in describing all the known gravitational phenomena at that time. The first deviation from the Newtons theory was noticed in the precession of Mercurys orbit; a 43 arc-seconds per century excess precession over that given by Newtons theory was observed. However, not because of such small deviation in just one experimental results, Einstein developed General relativity to make the theory of gravitation consistent with Special Theory of Relativity (STR).

Newtonian mechanics is based on the existence of absolute space and thereby absolute motion whereas STR rests on the idea that all (un-accelerated) motions are relative in nature. A consequent feature emerges in STR that no information can be transmitted with speed greater than the speed of light whereas the Newtons law of gravity implies action at a distance i.e. in Newtonian paradigm the gravitational information moves with infinite speed. In order to have a gravitational theory consistent with the under-lined philosophy of STR, Einstein developed GR that eventually explains the excess precession of Mercurys orbit over the Newtonian theory and matched as well as other experimental findings [Weinberg, 1972, Misner et al., 1973].

GR is geometrized theory of space time in which gravity is not regarded as a force (in the conventional sense) rather it is a manifestation of curved spacetime. The theory is guided by Mach's principle that advocates for relativity of all motion including rotational/accelerated motion. Besides the theory is based on mainly two fundamental principles, namely the Equivalence principle and the Principle of General Covariance [Weinberg, 1972, Coley and Wiltshire, 2017]. The former principle

demands for the exact equivalence of inertial mass and gravitational mass whereas the later principle states that the form of all physical equations should be the same in any arbitrary frame of reference. A clever and standard approach of satisfying the Principle of General Covariance is to write the equations in tensorial form that ensures form invariance under general coordinate transformation.

The GR can be framed through Einstein-Hilbert action [Hooft, 2001] which is given by

$$S_{\rm EH} = \int \mathrm{d}^4x\sqrt{-g}\left(\frac{Rc^4}{16\pi G} + \mathcal{L}_{matter}\right), \tag{1.1}$$

where the factor $\sqrt{-g}$ is invariant under coordinate transformations, R the Ricci scalar and $S_{matter} = \int \mathrm{d}^4x(\sqrt{-g}\mathcal{L}_{matter})$ represent the action of various matter fields. Varying $S_{\rm EH}$ with respect to the metric one gets the Einstein field equations

$$G_{\mu\nu} = -\frac{8\pi G T_{\mu\nu}}{c^4}, \tag{1.2}$$

where $T_{\mu\nu}$ is the energy-momentum tensor for matter and $G_{\mu\nu} = R_{\mu\nu} - \frac{1}{2}g_{\mu\nu}R$ is the Einstein tensor, $R_{\mu\nu}$ is the Ricci tensor and and $g_{\mu\nu}$ is the metric tensor respectively.

There is a room to include a cosmological constant Λ in the Einstein-Hilbert action (1.1) without introducing new degrees of freedom. In this case, the action is

$$S_{\rm EH} = \int \mathrm{d}^4x\sqrt{-g}\left(\frac{(R-2\Lambda)c^4}{16\pi G} + \mathcal{L}_{matter}\right) \tag{1.3}$$

which yields the modified equation

$$G_{\mu\nu} = -\frac{8\pi G T_{\mu\nu}}{c^4} - \Lambda g_{\mu\nu}. \tag{1.4}$$

The field equations are formulated respecting the Bianchi Identity that ensures that the energy-momentum is a conserved quantity.

1.3 Experimental tests of General Relativity

Since its formulation by Einstein, GR has been probed by a variety of experiments with increasingly high precision and GR has passed all such tests conducted till now. However, the theory has been tested so far mainly in the weak field regime and except the recent detection of gravitational waves by LIGO [Turyshev, 2016], GR remains untested in the strong field environment.

For tests in the weak field regime Parametrized Post Newtonian (PPN) [Poisson and Will, 2014] formalism is usually employed that covers any possible deviations from the GR space time.

In the weak and slow motion, the space-time metric predicted by most of the theory of gravitation has the same structure and they are expressed by an expansion about the well-known Minkowski metric (g_{ij}) in terms of some dimensionless small gravitational potential (U, ψ, φ).

$$g_{00} = -1 + 2U - 2\beta U^2 + 4\psi - \zeta\varphi \tag{1.5}$$

$$g_{ij} = \delta_{ij}(1 + 2\gamma U) \tag{1.6}$$

Where,

$$U(x,t) = \int \frac{\rho(x^{'},t)}{|x-x'|} d^3x' \tag{1.7}$$

$$\Psi(x,t) = \int \frac{\rho\left(x^{'},t\right)\psi(x^{'},t)}{|x-x'|} d^3x' \tag{1.8}$$

$$\psi = \beta_1 \overrightarrow{v}^2 + \beta_2 U + \frac{1}{2}\beta_3 \Pi + \frac{3}{2}\beta_4 P/\rho_0 \tag{1.9}$$

$$\varphi\left(x,t\right) = \int \frac{\rho(x^{'},t)}{|x-x'|^3}\left[(\overrightarrow{x} - \overrightarrow{x}').\overrightarrow{v}(x^{'},t)\right]^2 d^3x' \tag{1.10}$$

$$\Pi = \frac{\rho_0 - \rho}{\rho} \tag{1.11}$$

Here P is the pressure and $\overrightarrow{v}(x^{'},t)$ represents velocity of matter in the solar system, the constants $\gamma, \beta, \beta_1, \beta_2, \beta_3, \beta_4$ and ζ. If we consider the rotating parts also, then, ten parameterized post-Newtonian (PPN) parameters $\gamma, \beta, \beta_1, \beta_2, \beta_3, \beta_4$, $\zeta, \Delta_1, \Delta_2$ and η are sufficient to complelely characterizing the weak-field behaviour of a wide class of metric theories of gravity which includes general theory of relativity.For GR the parameters $\gamma = \beta = \beta_1 = \beta_2 = \beta_3 = \beta_4 = \Delta_1 = \Delta_2 = 1$ and other PPN parameters $\zeta = \eta = 0$.

It may be noted that there are two type of notations , the above notation are termed as notation of Will [Will, 1971, Ni, 1972] and [Misner et al., 1973] as in table 1.1. There is another notations to present PPN parameters termed as Alpha-zeta notation, the relation between Alpha-zeta notation and old notation of [Will, 1971] is given in table 1.2 . In this notation, α_1, α_2 and α_3 parameters measure

Table 1.1: *PPN Parameters and What they represents*

Parameter	Physical Significance
γ	How much space curvature g_{ij} is produced by unit rest mass ?
β	How much nonlinearity is there in the superposition law for gravity g_{00} ?
β_1	How much gravity is produced by unit kinetic energy $\frac{1}{2}\rho_0 v^2$?
β_2	How much gravity is produced by unit gravitational potential energy ρ_0/U ?
β_3	How much gravity is produced by unit internal energy $\rho_0\Pi$?
β_4	How much gravity is produced by unit pressure P ?
Δ_1	How much dragging of inertial frames g_{0j} is produced by unit momentum $\rho_0 v$?
Δ_2	Difference between radial and transverse momentum on dragging of inertial frames
ζ	Difference between radial and transverse kinetic energy on gravity
η	Difference between radial and transverse stress on gravity

Table 1.2: *Relationship between Alpha-zeta notation and old notation*

Alpha-zeta notation
$\gamma = \gamma$
$\beta = \beta$
$\alpha_1 = 7\Delta_1 + \Delta_2 - 4\gamma - 4$
$\alpha_2 = \Delta_2 + \zeta - 1$
$\alpha_3 = 4\beta_1 - 2\gamma - 2 - \zeta$
$\zeta_1 = \zeta$
$\zeta_2 = 2\beta + 2\beta_2 - 3\gamma - 1$
$\zeta_3 = \beta_3 - 1$
$\zeta_4 = \beta_4 - \gamma$
ξ is calculated from $3\eta = 12\beta - 3\gamma - 9 + 10\xi - 3\alpha_1 + 2\alpha_2 - 2\zeta_1 - \zeta_2$

the extent of and nature of "preferred frame effects" [Misner et al., 1973] whereas $\zeta_1, \zeta_2, \zeta_3, \zeta_4$ and α_3 measure the extent of and nature of breakdowns in conservation of energy (4 laws), momentum and angular momentum (6 laws). Any theory with $\zeta_1 = \zeta_2 = \zeta_3 = \zeta_4 = \alpha_3 = 0$ is called a conservative theory. The general relativity and the Dicke-Brans-Jordon theory are conservative theories with no prefered-frame effects.

In terms of this notation, general relativity has PPN parameters $\gamma = \beta = 1$ and $\alpha_1 = \alpha_2 = \alpha_3 = \zeta_1 = \zeta_2 = \zeta_3 = \zeta_4 = \xi = 0$. Out of all the parameters, β and α are in some sense very important. They are the usual Eddington-Robertson-Schiff parameters used to desscribe the classical tests of general relativity.

1.3.1 The Classical tests of General Relativity:

Bending of light

The theory of GR predicts the deflection of light in the presence of mass distribution. In astrophysical situation, a light ray or a photon originating from some distance source (say stars) approaches the solar system (or sun) along an asymptotic straight line (say AB) will be deflected from its normal path to another asymptotic straight line (BC) through a very small amount 1.1.

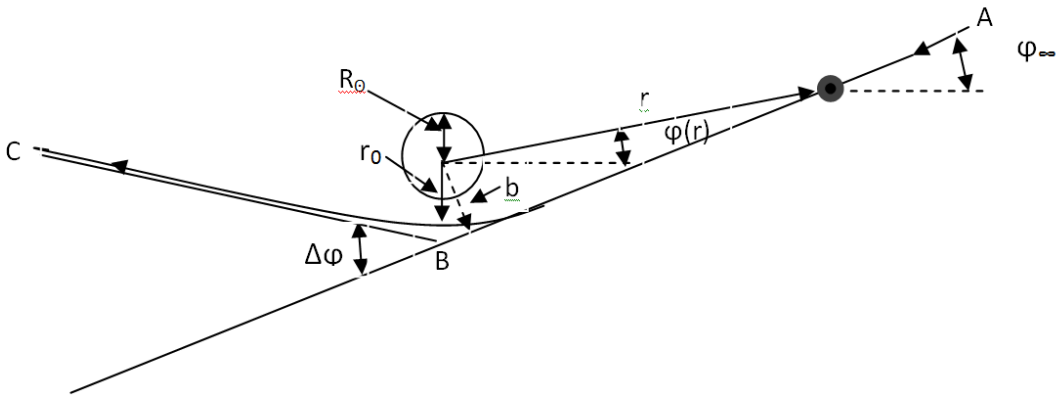

Figure 1.1: Deflection of light by the sun

$$\Delta\varphi = 2\left|\varphi\left(r_0\right) - \varphi_\infty\right| - \pi \tag{1.12}$$

If this angle $\Delta\varphi$ is positive, the trajectory is bent towards the sun; if this angle $\Delta\varphi$ is negative then the trajectory is bent away from the sun.

$$\varphi\left(r_0\right) - \varphi_\infty = \int_r^\infty \sqrt{A(r)}\left[\left(\frac{r}{r_0}\right)^2\left(\frac{B(r_0)}{B(r)}\right) - 1\right]^{-1/2}\frac{dr}{r} \tag{1.13}$$

Considering the first order in MG/ ($c^2 r_0$), the deflection angle thus becomes

$$\Delta\varphi = \frac{4MG}{r_0 c^2}\left(\frac{1+\gamma}{2}\right) \tag{1.14}$$

For light ray deflected by the sun, $M = M_{\odot} = 1.97 \times 10^{33} g$, $\frac{MG}{c^2}$=1.475 km, the minimum value of r_0 is $R_0 = 6.95 \times 10^5 km$, so

$$\Delta\varphi = \frac{R_0}{r_0}\theta_0 \tag{1.15}$$

Where $\theta_0 = \frac{4MG}{R_0}\left(\frac{1+\gamma}{2}\right) = 1.75"\left(\frac{1+\gamma}{2}\right)$

For GR, $\gamma = 1$, so it predicts a deflection toward the sun $\theta_0 = 1.75"$ which is confirmed by the observations with a high accuracy.

For Brans- Dicke theory the expression for $\theta_0 = \frac{4MG}{R_0}\left(\frac{2w+3}{2w+4}\right)$

Physical consequence of bending of light: -

If one distance object is in front or close to another more distance object, then, the more distant object may show the effects of gravitational lensing. These effects may include:-

1. Einstein rings and arcs: Here the more distant object's light appearing as ring.
2. Microlensing:-Brightening of a more star due to the focusing effects
3. Multiple views of the same object e.g. Quasars

Present experimental status:

Eddington and his co-workers performed the first successful experiment (with 30% accuracy) to confirm bending of light as proposed by Einstein. Until, the development of radio interferometry and Very-Long-Base radio interferometry (VLBI),

succeeding experiments were not much better with low accuracy. However, VLBI produced improved determinations of the deflection of light as these experiments have capability of measuring angular separations in order of the 100 microsecond or less. The frequent astronomical observation of quasi-stellar radio sources passing close to the sun helped a lot. A 1995 VLBI measurement using the quasar source like 3C273 and 3C279 yielded $\gamma - 1 = (-8 \pm 34) \times 10^{-4}$ [Will, 2014, Lebach et al., 1995], while a 2009 measurement using the same two quasars plus two nearby radio sources yielded $\gamma - 1 = (-2 \pm 3) \times 10^{-4}$ [Will, 2014, Fomalont and Kopeikin, 2003]. Recent, transcontinental and intercontinental VLBI observations of a larger number of quasars and radio galaxies have been done to monitor the Earth's rotation. As, these measurements are sensitive to the deflection of light over the entire celestial sphere (at 90^o from Sun). In 2004, an analysis of almost 2 million VLBI observations of 541 radio sources at 87 sites yielded yield $\gamma - 1 = (-1.7 \pm 4.5) \times 10^{-4}$ [Will, 2014, Shapiro et al., 2004] where the analysis incorporating data through 2010 yielded $\gamma - 1 = (-0.8 \pm 1.2) \times 10^{-4}$ [Will, 2014, Lambert and Le Poncin-Lafitte, 2009].

Through Sloan Digital Sky Survey (SDSS) the data were collected for gravitational lensing by 15 elliptical galaxies, which helped to have remarkable measurement of γ on galactic scales in 2006. Comparing the observed lensing with the lensing produced by the models provided a 10% bound [Will, 2014], in agreement with relativity. Unlike, the much tighter bounds as described, this bound was on a galactic scale.

1.3.2 Precession of the perihelion

The celestial mechanics of general relativity differs from that of classical mechanics. Due to this, we get non-Newtonian periapsis precession i.e. the apsides of orbits precess more than what is expected under Newton's theory of gravity. These orbital effects due which the orientation of planets orbit is found to precess with time, is commonly term as "Precession of the perihelion".

For the PPN metric, the relativistic expression of precession of the perihelion in radian per revolution for precession is given by

$$\Delta\varphi = \frac{6MG}{L\ c^2}\left[\left(\frac{2-\ \beta+2\gamma}{3}\right)+\frac{1}{6}\ \ (2\alpha_1-\alpha_2+\alpha_3+2\varsigma_2)\,\eta+\frac{J_2R^2c^2}{2MGL}\ \right] \tag{1.16}$$

Where $L = a(1-e^2)$ is the semi-latus rectum of the orbit with the semi major axis 'a' and the eccentricity e, M=M_1+M_2 is the total mass of the two body system, $\eta = \frac{M_1M_2}{M^2}$ = reduced mass of the system, $J_2 = \frac{(C-A)}{m_1R^2}$ [Mecheri et al., 2004], where C and A are the moments of inertia about the body's rotation and equatorial axes, respectively.

Substituting standard orbital elements for Mercury and the Sun, we obtain the precession in seconds of arc per century for fully conservative theory of gravity as,

$$\Delta\varphi = 42.98\text{"}\left[\left(\frac{2-\ \beta+2\gamma}{3}\right)+3\times10^{-4}\frac{J_2}{10^{-7}}\ \right] \tag{1.17}$$

Present Experimental Status:-

The first successful observation of Mercury was made long back to 1765 and these data were reanalyzed by Clemence in 1943, he finds $\Delta\varphi = 43.03\text{"}\ \pm0.45\text{"}$ per century and is in excellent agreement with general relativity.

The recent fits (2014) of planetary data including data from the Messenger spacecraft that orbited Mercury significantly improve the knowledge of Mercury's orbit. Adopting the Cassini bound on γ a priori; these analyses yield a bound of β given by $\beta - 1 = (-4.1 \pm 7.8) \times 10^{-5}$ [Konopliv et al., 2011].

1.3.3 Shapiro Effect (also known as gravitational time delay)

The curvature of the space-time surrounding a massive body like Sun increases the travel time of light rays relative to what it would be the case in flat space. As such, light signal takes longer than expected to move through a gravitational field.

The time required by the light to move from r to r_0 in a gravitational field is described by

$$ct\,(r, r_0) \cong \sqrt{r^2 - {r_0}^2} + (1+\gamma)\,\frac{MG}{c^2} ln\left(\frac{r + \sqrt{r^2 - {r_0}^2}}{r_0}\right) + \frac{MG}{c^2}\sqrt{\left(\frac{r - r_0}{r + r_0}\right)} \quad (1.18)$$

In the above equation, the leading term is just the time required by light to travel in flat space from point r to r_0. The other terms are a general-relativistic delay in time.

For r$\approx r_0$, the case like when mercury is at superior conjunction and the radar signal just gazes sun, the maximum round trip excess time delay is given by

$$c\Delta t_{max} \approx 5.9\ km\ \left\{1 + 11.2\left(\frac{1+\gamma}{2}\right)\right\} \quad (1.19)$$

For GR, $\gamma = 1$, so it predicts that the maximum excess time delay will be $\Delta t_{max} \approx 72\ km$ or $\Delta t_{max} = 240 \mu sec.$

The main experimental hurdle is that the radar signal in not reflected from just one point on Mercury's Surface, but rather comes from a good-sized area, and is spread out in arrival time by several hundred microseconds. To overcome this problem, Shapiro's used a technique termed as "delay-Döppler mapping". This technique involves knowledge of reflecting properties of the surface of mercury and also involves measuring the distribution of the return signal power in frequency as well as arrival time.

Another more fundamental difficulty is that in order to compute an excess time, is that we need to know the time that the radar signal would take in absence of Sun's gravitation. That is, we have to know the distance

$$\sqrt{{r_E}^2 - {r_0}^2} + \sqrt{{r_M}^2 - {r_0}^2}$$

to within 1.5 km!. But with Optical astronomy alone, it is not possible to know the locations of the centre of Mercury or the Earth or Mercury's radius to the needed accuracy. Shapiro's group deals with this problem by obtaining theoretical models, in which the distance r_E , r_M and r_o are calculated using GR in term a set of unknown parameters, including β, γ, $GM_\odot/c^2$, the equatorial radius of Mercury, and the positions and velocities of Mercury and the earth at some initial time. Theses parameters were then determined by fitting the observed radar travel times to Mercury and back with theoretical formulas.

Present Experimental status:

Using the 7840 MHz Haystack radar at Lincoln Laboratory during the superior conjunctions of mercury (1967) gave good agreement between theory and observation. With improvements in data analysis, the result improved to $\gamma - 1 = (1.03 \pm 0.1) \times 10^{-4}$.

In 1970, Shapiro reanalyzed older optical observation of the sun, moon and planets in conjunction with the new radar data and finds that the quadruple term in the sun's gravitational potential has the value $J_2 = (-8 \pm 34) \times 10^{-4}$.

According to Dicke and Goldenberg, the corresponding term bound is $J_2 = (2.7 \pm 0.5) \times 10^{-4}$ from the solar oblateness data. If this term is constrained to vanish, then according to Shapiro's analysis, there will be extra precessions of the perihelia of the Mercury and Mars orbits which are 0.99 ± 0.01 and 1.07 ± 0.1. Shapiro also proposed the measurement of the time delays in the arrival of radio pulses from pulsars and corresponding to approach of pulsar CP0952 within 5^o of the sun, the radio pulses would be delayed by about 50 μsec. In 1970,a group at Jet Propulsion Laboratory measured a series of time delays of radar signals from earth to transponders placed in the artificial satellites Mariner 6 and 7 and thence back to earth. Analysis of those data gives a time delay within 5 % of that predicted by general relativity. But, these experiments has drawbacks as the radar frequencies used were in S-band, about 2300 Mhz where the solar corona played a troublesome role, further, the mariner satellites were small enough and are appreciably affected by non-gravitational forces (Solar radiation pressure, gas leakage and thrust imbalances).

A significant improvement in result was reported in 2003 from Doppler tracking of the Cassini spacecraft to Saturn [Bertotti et al., 2003], with the result

$$\gamma - 1 = (2.1 \pm 2.3) \times 10^{-5}$$

This is possible due to the ability to do Doppler measurement (which is essentially the measuring of the time derivative of the Shapiro delay) using both X-band and Ka-band radar, thereby significantly reducing the dispersive effects of the solar corona.

In addition to this 2002 superior conjunction of Casini was particularly favourable: with space-craft at 8.43 AU from the sun, the distance of closest approach of the radar signals to the Sun was only 1.6 $R_{\odot}$.

1.3.4 Geodetic precession and Lense-Thirring effect

Besides the classical solar system tests and binary pulsar tests of gravity, two other weak field tests of GR through two gravitational effects, namely geodetic effect and the frame-dragging or Lense-Thirring effect have been conducted recently by Gravity Probe-B mission. According to GR, a top such as the spinning Earth in curved space time, due to curvature effect, the spin axis precesses which is the geodetic precession. Note that here the precession is with respect to remote celestial objects those from mean rest frame of the Universe. The effect is small, proportional to $1 + 2\gamma$ (γ is the 1st PPN parameter). The Lense-Thirring effect is the GR effect on the precession of a gyroscope under the influence of a nearby rotating mass. Essentially it is a frame dragging effect. The Lense-Thirring effect depends on the factor $1 + \gamma + \alpha_1/4$, where α_1 is a preferred frame parameter that allows possible dependency on motion relative to the remote celestial objects. Gravity Probe B is NASA satellite based mission to test Einstein's gravitational theory. The mission carried four Gyroscopes and a cryogenic optical telescope. The later was used to track a guide (reference) star thereby establishing the inertial reference frame. The curvature of space time induced by the Earth exerts a torque on the gyroscope resulting precession of its axis by about 6.6 arcseconds per year in the plane of satellite. Besides, the spin of the Earth also employs a torque on the gyroscope leading to precession of the gyros

axis by about 0.39 arcseconds per year in perpendicular to the orbital plane. The findings of Gravity Probe B confirmed both predictions of GR: the geodetic effect to a precision of 0.3% and frame-dragging to 20% [Everitt et al., 2011].

1.4 Moderately strong/strong field Tests:

It involves the following tests: Binary pulsar test, Gravitational-Wave Test, Astrophysical and Cosmological tests

1.4.1 Binary pulsar test

Binary Pulsar PSR 1913+16

In year 1974, Joe Taylor and Russel Hulse discovered binary pulsar PSR 1913+16 [Hulse, 1994]during a routine search for new pulsars. The binary pulsar consists of two neutron stars with masses 1.438 and 1.390 solar masses with orbital period $P_b = 0.3229974489d$, with projected semi-major axis $x = 2.34177s$ and eccentricity $e = 0.617134$. Further the orbits are very close ($\approx 1R_{\odot}$) and there is no evidence of mass transfer from the companion with evolutionary arguments [Antoniadis et al., 2013] suggest that the companion is dead star while 1913+16 is a "recycled" pulsar [Narayan et al., 1991]. The result is that the orbital motion is very clean; free from tidal and other such effects as observed during data acquisition with intrinsic stability of the pulsar clock with the atomic time using GPS (except few small "glitch" as observed in May 2003).This configuration makes the binary pulsar one of the most important relativistic objects of our galaxy. The observational parameters that are obtained from least-squares solution of the arrival-time data fall into three groups:

1. Non-orbital parameters: e.g. Pulsar period, declination, derivative of period, Right ascension

2. Keplerian parameters: Projected semi-major axis, eccentricity, orbital period, longitude of periastron, Julian date of periastron.

3. Post-Keplerian parameters: Mean rate of periastron advance, redshift, orbital period derivative

This configuration makes the binary pulsar one of the most favoured objects in our galaxy to confirm validity of general relativity [Wex, 2014, Weisberg and Huang, 2016] . Binary pulsar are directly or indirectly are test bench to test a number of relativistic parameters such as quadratic Doppler effects, gravitational red shift, anomalous precession of the periastron, the Shapiro time delay etc.

Further, with the consistency among the constraints suggest that the two bodies behaviour as point masses without complicated tidal effects, obeying the general relativistic equations of motion including gravitational radiation is also a test of strong gravity, in which the internal structure of the neutron stars does not influence their orbital motion, as predicted by the Strong Equivalence Principle of GR. Also, the observations suggest that the pulse profile is varying with time suggest that the pulsar is undergoing geodetic precession on a 300-year timescale as it moves through the curved space-time generated by its companion, the same is consistent with GR, assuming that the Pulsar's spin is suitably misaligned with the orbital angular momentum.

Double Pulsar J0737-3039A

J0737-3039A binary pulsar system was discovered in 2003 having very short orbital period (0.1 days) and large periastron advance (16.8995^o per year) with pulsar as companion [Will, 2014]. For these case, the two projected semi-major axes could be measured, thereby it is very easy to obtain mass ratio from the two values of projected semi-major axes ($a_p \sin i$). The two masses $m_A = 1.3381 \pm 0.0007 M_\odot$ and $m_B = 1.2489 \pm 0.0007 M_\odot$ have been obtained by combining the ratio with the periastron advances, assuming GR, where A denotes the first pulsar and B denote the second pulsar. The measured result assuming GR and observational data almost overlap. Further, due the location of the system, galactic proper-motion effects play a significantly smaller role in the interpretation of $\dot{P}_b$ measurements in compare to PSR 1913+16. The geodetic precession of pulsar B's spin axis has been measured by monitoring changes in the patterns of eclipses of the signal from pulsar A, with in agreement with GR to about 13 percent [Breton et al., 2008].

1.4.2 Gravitational waves

In 1916 Albert, Einstein predicted the existence of Space-time curvature generated by mass-energy propagating with speed c on a flat and empty space-time, the gravitational waves [Einstein and Rosen, 1937]. According to Einstein, the linearized weak-field equations had wave solutions, transverse in nature that travel at the speed of light, usually generated by temporal variations of the mass quadrupole moment of the source [Thorne, 1980]. Landau and Lifshitz in 1941 showed the emission of gravitational waves by a self-gravitating system of slowly moving bodies [Will, 2014]. Hermann Bondi in year 1957 on the basis of a Gedanken experiment showed that

gravitational waves do carry energy .Experiments to detect gravitational waves began with resonant mass detectors developed by Weber in 1960 [Weber, 1960], that was followed by international network of cryogenic resonant detectors [Astone et al., 1993]. Interferometric detectors were first suggested in early 1960s and in 1970s. The detail study of the noise, performance and throughputs to improve output led to a proposal for long baseline broadband laser interferometer with increased sensitivity. By 2000s, a many operational detectors were developed like TAMA 300 in Japan, GEO 600 in Germany, the Laser interferometer Gravitational-Wave Observatory (LIGO) in the United States, and VIRGO in Italy. By 2011, a global network is setup for joint observations. In 2015, advanced LIGO became functional with financial support of U.S. National Science Foundation in which three gravitational wave interferometers were upgraded to make it more sensitive.

The existence of gravitational waves predicted by General Relativity has been verified by observing the rate of energy loss, due to the emission of gravitational radiation in pulsar PSR B1913+16 in 1974 and double pulsar PSR J0737-3039A/B in 2003. They are important as the mean rate of periastron advance of binary pulsar (PSR B1913+16) is $\Delta\varphi = 4.226598^o$ per year and for double pulsar (PSR J0737-3039A/B) is very high $\Delta\varphi = 16.89957^o$ per year as compared to Mercury which is about $\Delta\varphi = 43.03$" per century. The better thing about the system is that both the neutron stars being pulsar, we have an abundant amount of timing data; which allowed multiple GR tests (quadratic Doppler effects, the gravitational red shift, Shapiro gravitational time delay, the decay of orbital time period due to emission of gravitational waves and many more) in one system [Weisberg and Huang, 2016].

After that the relativistic theory of motion of the binary pulsars has been developed by a number of authors. The same helped a lot to develop a library of templates (called numerical relativity) of gravitational waves from the coalescing binary black holes which further helped in direct detection of the transient gravitational waves signal by two detectors of the Laser Interferometer Gravitational-Wave Observatory (LIGO) simultaneously on September 14, 2015 at 09:50:45 UTC. It matched with the waveform as predicted by GR for the in-spiral and merger of a pair of black holes and ring-down to a single black hole [Abbott et al., 2016].

1.4.3 Astrophysical Tests

It is very difficult to test GR in strong-field regime due to uncertain physics. In the solar system test and weak field regime, the gravitational effects as well as non-gravitational effects can be measured cleanly and separately. The nature is always not like that in strong-field. But, under some suitable condition, we can have qualitative and quantitative strong-field tests of GR. Such as binary pulsars and space-time near black holes . The studies of special type of accretion process termed as advection-dominated accretion flow in low luminosity binary X-rays sources yield the signature of the black hole and its event horizon. The spectrum of frequencies from galactic black holes binaries, spectral shapes of iron fluorescence lines [Reynolds, 2013, 2014] from the inner regions of accretion disks and accretion luminosity helps to understand the space-time geometry very close to the black hole [Doeleman et al., 2009]. Apart from this, many binary pulsars permit precise measurements of gravitational

phenomena in strong-field context due to cleanliness of the system.

1.4.4 Cosmological Tests

Cosmological observations also provide strong experimental confirmation on General relativity. The evolution of the Universe is governed by gravity and therefore is described by GR as the (standard) theory of the Universe. Assuming that the Universe is isotropic and homogenous at large scales and the space is filled uniformly with matter, the GR field equations lead to the so called Friedmann-Lemaitre-Robertson-Walker solution (also known as Friedmann-Einstein model). As per the model the Universe was created in a big explosion (big bang) about 15 billion years ago (hereby the model is also as big bang cosmology) and it is dynamic in nature.

However, it was commonly believed until 1931 that Universe is static. So Einstein forcefully introduced a constant (known as cosmological constant) in his field equations to ensure that his theory leads to a static universe. However, it was soon realized that Einsteins static Universe is unstable and Lematre concluded that the Universe should be expanding rather than remaining static. The expansion feature of the Friedman-Einstein model should reveal from predicted cosmological redshift of distant galaxies that should increase with distance. In 1929, Hubbles analysis of redshifts of galaxies and their distance data found in an astronomical observations by Slipher confirmed the expansion paradigm of GR based cosmological model. Another landmark prediction of the big bang cosmology is the existence of relic Cosmic Microwave background radiation (CMBR) which is a black body radiation of temperature around 5 degree Kelvin . The discovery of CMBR in 1964 by Penzias and

Wilson provides a strong evidence in favour of Big Bang cosmology and GR. The success of Big Bang cosmology to explain the present day nuclear abundances through nucleosynthesis [Will, 1993] is another success for the Friedman model and GR.

The cosmological expansion is caused by initial explosion but due to gravitational attraction the universe should start collapsing at a point of time. But the recent findings show something else. In the year 1998, two independent teams concluded after analysing their observed data on distance and redshifts of Type Ia supernovae that the Universe is not only expanding but the expansion is accelerating [Peebles and Ratra, 2003]. To explain such feature in the framework of GR, the Universe has to be filled by a new energy-momentum component with negative pressure and nearly constant energy density i.e. by so called dark energy. One possibility is that dark energy is Einsteins cosmological constant though its theoretical interpretation is problematic.

A combination of very different observational probes now suggest that in the present Universe about 68% of the total energy density is dark energy, about 27% dark matter and only the remaining 5% is made of by the normal matter. The big bang cosmology with Cold Dark Matter and Λ (ΛCDM) paradigm has emerged as the standard model of cosmology.

1.5 Objectives of the thesis

GR has been tested and confirmed mainly in the weak field regime, the theory remains essentially untested not only in the strong-field regime but also in the intermediate field strength domain. The effect of rotation on space time has also not

been confirmed experimentally. Some well-motivated alternative theories of gravity, such as the scalar-tensor theories, are also compatible with all the weak field tests but differ from GR at higher parameterized post-Newtonian (PPN) orders and in strong field regime. One of the outstanding debatable issues relating to gravity, is to ascertain whether the end state of gravitational collapse in our physical Universe renders black hole (BH) or naked singularity. There is also issues about the end state of gravitational collapse in our physical Universe and physical reality of naked singularity solutions. Thus exploring the strong/moderately strong filed effects of gravitational theories, both theoretically as well as experimentally, is of prime importance in the present day gravitational research.

More importantly GR cannot explain the recent observations on large astronomical/cosmological scales unless an exotic nearly homogeneous energy density with negative pressure, the so called dark energy and also a non-luminous unseen matter, the so called dark matter are invoked as dominant components of the matter content of the Universe.

A diverse range of results , from cosmic microwave background temperature fluctuation measurements [Bennett et al., 1996] to high-redshift supernova measurements [Perlmutter et al., 1999], baryon acoustic oscillation measurements and weak lensing techniques (such as cosmic shear and red-shift space distortion), together firmly suggest that the universe is nearly, if not exactly, flat and is undergoing a phase of accelerating expansion. The accelerated expansion is usually explained in the framework of GR in terms of the dark energy, whose dominance over matter at late eras is held responsible for the Universe acceleration. It is interesting to ask whether the

dark energy could have significant effects at local scale. It is already known from various recent studies that the observable effects of the cosmological constant, which is considered as the most viable candidate for the dark energy, on the Solar system and double pulsars gravitational phenomena are too small to be detected in the near future. But the effect of cosmological constant could be important for extended galaxy clusters. For instance, the contribution of cosmological constant on bending of light could be significant, larger than the second order term, for many lens systems such as cluster of galaxies [Ishak et al., 2008].Several aspects of influence of dark energy on local gravitation are, however, not thoroughly investigated yet. As for example, the importance of the study of photon trajectories from the reference objects in bending and other concerned calculations are often ignored; when such an aspect is taken into consideration the contribution of cosmological constant to the effective bending is found to depend on the distances of the source and the reference objects [Bhadra et al., 2010]. Similarly to look for the effect of dark matter on various gravitational phenomena is also imperative.

Under the context, the objectives of the proposed thesis work are mainly the following:

a) From theoretical consideration we would look for observable effects of gravitation and the effects due to dark matter and dark energy. We shall particularly study gravitational time delay of particles with non-zero mass and explore how the phenomenon can be exploit to probe higher order effects of gravity as well as effects of dark matter/energy.

b) The relativistic accretion phenomena around Black holes (BHs)/compact mas-

sive objects offers a testbed for probing gravity in the strong-field regime. The study of accreting BH systems involves solving general relativistic (GR) hydrodynamic/ magnetohydrodynamic (MHD) equations in a strong gravitational field regime. Owing to the complex and nonlinear character of the underlying equations in GR regime, analytical/quasi numerical treatment of the problem is virtually discarded. Even numerical simulation is complicated by several issues such as different characteristic time scales for propagating modes of general relativity and relativistic hydrodynamics. A useful and clever technique to treat accretion and its related processes around BHs using hydrodynamical/MHD equations in the Newtonian framework by using some pseudo-Newtonian potentials (PNPs) which are essentially modification of Newtonian gravitational potential developed with the objective to reproduce (certain) features of relativistic gravitation. Adopting PNPs, one can comprehensively construct more realistic accretion flow models in simple Newtonian paradigm, while the corresponding PNP would capture the essential GR effects in the vicinity of the compact objects.

The prevailing PNPs lay emphasize mostly to reproduce marginally stable and marginally bound orbits. But in general, they are unable to reproduce observationally verified weak field tests in general relativity like geodetic precession, gravitational bending of light or gravitational time delay. One of the main objective of the present thesis is to develop PNPs corresponding to different well known space time metrics those can reproduce almost all of the corresponding GR features with good accuracy. Subsequently we would estimate some observable effects in strong/moderate strong field regime such as angular momentum, radial velocity epicyclic frequency of test particle motion in the vicinity of black holes, the nature of elliptical like trajectory of

particle orbit, eccentricity etc. Finally we shall study the effects of spin, naked singularity, cosmological constant etc on accretion. Here note that for tests in the weak field regime parametrized post Newtonian (PPN) formalism is usually employed that covers any possible deviations from the GR space time. However, no such general formalism exists for strong field tests. We, therefore, consider different well known space time metrics, which include Schwarzschild de Sitter solution that describes static spherically symmetric exterior space time in an accelerating universe, Kerr metric that describe gravitational field of spinning massive object, Janis-Newman-Winicour solution that describes a naked singularity solution, separately in our strong/moderately strong field study.

c) We shall also analyze the x-ray astronomical data obtained with the Rossi X-ray Timing Explorer (RXTE) and XMM Newton to extract information regarding nature of compact objects (black hole etc) and emission processes which may give some confirmation of the gravitational theories.

The plan of the thesis is the following.

In the next chapter, the effect of several dark energy models on gravitational time delay of particles with non-zero mass are investigated upto first order accuracy. Also, the expressions for gravitational time delay under the influence of conformal gravity potential that we describes the flat rotation curve of spiral galaxies is derived. At the end we have reported how to discriminated between conformal gravity description of dark matter and normal dark matter using gravitational time delay observations.

In chapter 3, we have studied the effect of cosmological constant on orbital dynamics as well as on accretion. For doing the same, we obtain three dimensional analogous

Newtonian like potential in spherical geometry corresponding to Schwarzschild-de Sitter (SDS) space time. Subsequently, we applied the derived potential to study the effect of cosmological constant on sonic radius as well as Bondi accretion rate, specially for spherical accretion with lower adiabatic constant and temperature.

In chapter 4, , we have formulated a generic Newtonian like analogous potential correspond to a claas of static general relativistic spacetime, and subsequently the derived potentials correspond to Janis-Newman-Winicour (JNW) and Reissner-Nordstrom (RN) spacetimes applied to circumvent complex GR framework for the study of orbital dynamics and stationary accretion phenomena around a naked singularity.

In chapter 5, we have obtained PNP for the Kerr space time in low energy limit that reproduces all general relativistic features with good accuracy unlike any other texisting PNPs for Kerr space time. Using the derived potential, we have subsequently studied the particle dynamics and the effect of spin on the radiation flux and efficiency in case of a stationary accretion.

In chapter 6, we have constructed a self-consistent and an exact relativistic Newtonian analogue corresponding to a general class of gravitational static spherically symmetric metric staring directly from a generalized scalar relativistic gravitational action in Newtonian framework, that gives geodesic equations of motion identical to those of the parent metric. This relativistic analogous potential is expected to be quite useful in studying wide range of astrophysical phenomena in strong field gravity, like black hole (BH) accretion, tidal disruption of a star by a supermassive BH (SMBH), or in binary mergers, or analyzing galactic dynamics around SMBH, and

can even be tested in other applications of gravity as well.

In chapter 7, we have reported the first detection of (negative) spectral lags in the X-ray emission below 10 keV from the gamma ray binary $LSI + 61^o$ 303 during large flaring episodes using the Rossi X-ray Timing Explorer (RXTE) observations. The possible cause of the observed spectral lag features have been discussed.

We have finally concluded our results in chapter 8.